0026-895X/08/7404-1046–1058$20.00
MOLECULAR PHARMACOLOGY
Copyright © 2008 The American Society for Pharmacology and Experimental Therapeutics
Mol Pharmacol 74:1046–1058, 2008

Vol. 74, No. 4
44800/3379379
Printed in U.S.A.

The Induction of Orphan Nuclear Receptor Nur77 Expression by *n*-Butylenephthalide as Pharmaceuticals on Hepatocellular Carcinoma Cell Therapy

Yi-Lin Chen, Min-Hui Jian, Chai-Ching Lin, Jung-Cheng Kang, Shee-Ping Chen, Po-Cheng Lin, Putzer-Joseph Hung, Jen-Ren Chen, Wen-Liang Chang, Shinn-Zong Lin, and Horng-Jyh Harn

Graduate Institute of Biotechnology (Y.-L.C., M.-H.J.) and Department of Applied Animal Science (C.-C.L.), National Ilan University, Ilan, Taiwan, Republic of China; Division of Colon and Rectum Surgery, Department of Surgery, Buddhist Tzu-Chi General Hospital (J.-C.K.) and Institute of Medical Sciences (S.-P.C.), Buddhist Tzu-Chi University, Hualien, Taiwan, Republic of China; Department of Life Science and Institute of Biotechnology, National Dong Hwa University, Hualien, Taiwan, Republic of China (P.-C.L.); Department of Biochemistry, Brown University, Providence, Rhode Island (P.-J.H.); Division of Biotechnology, Agricultural Research Institute, Wufeng, Taichung, Taiwan, Republic of China (J.-R.C.); School of Pharmacy, National Defense Medical Center, Taipei, Taiwan (W.-L.C.); Center for Neuropsychiatry, China Medical University and Hospital, Taichung, Taiwan, Republic of China (S.-Z.L.); and Department of Pathology, China Medical University and Hospital, Taichung, Taiwan, Republic of China (H.-J.H.)

Received January 1, 2008; accepted June 23, 2008

ABSTRACT

N-Butylidenephthalide (BP), isolated from the chloroform extract of *Angelica sinensis*, has been examined for its antitumor effects on glioblastoma multiforme brain tumors; however, little is known about its antitumor effects on hepatocellular carcinoma cells. Two hepatocellular carcinoma cell lines, HepG2 and J5, were treated with either *N*-butylidenephthalide or a vehicle, and cell viability and apoptosis were evaluated. Apoptosis-related mRNA and proteins expressed, including orphan receptor family Nurr1, NOR-1, and Nur77, were evaluated as well as the effect of *N*-butylidenephthalide in an in vivo xenograft model. *N*-Butylidenephthalide caused growth inhibition of both the cell lines at 25 μg/ml. Furthermore, *N*-butylidenephthalide-induced apoptosis seems to be related to Nur77 translocation from nucleus to cytosol, which leads to cytochrome *c* release and caspase-3-dependent apoptosis. *N*-Butylidenephthalide-related tumor apoptosis was associated with phosphatidylinositol 3-kinase/protein kinase B (AKT)/glycogen synthase kinase-3β rather than the mitogen-activated protein kinase or protein kinase C pathway. Blockade of AKT activation enhanced proliferation inhibition and the induction of phosphor-Bcl-2 and Nur77 proteins. Besides, the increasing apoptosis by BP via transfection wild-type cAMP-response element-binding protein (CREB) into tumor cell was suppressed by dominant phosphorylation site mutation of CREB. This finding suggested CREB pathway was also partly involved in tumor apoptosis caused by BP. Administration of *N*-butylidenephthalide showed similar antitumoral effects in both HepG2 and J5 xenograft tumors. *N*-Butylidenephthalide induced apoptosis in hepatocellular carcinoma cells, both in vitro and in vivo, suggesting a potential clinical use of this compound for improving the prognosis of hepatocellular carcinoma cells.

This work was supported National Science Council of the Republic of China grants 96-2320-B-197-001-MY2 and 96-2320-B-303-001-MY3.

S.-Z.L. and H.-J.H. contributed equally to this work.

Article, publication date, and citation information can be found at http://molpharm.aspetjournals.org.

doi:10.1124/mol.107.044800.

Hepatocellular carcinoma (HCC) is one of the most frequent cancers worldwide. The main curative therapies for cancer are surgery and radiation, which, in general, are only successful if the cancer is diagnosed at an early stage. Cur-

ABBREVIATIONS: HCC, hepatocellular carcinoma; AS, *Angelica sinensis*; Nur77, nerve growth factor-induced B; NGF, nerve growth factor; PB, *N*-butylidenephthalide; AKT, protein kinase B; TCR, T-cell receptor; MAPK, mitogen-activated protein kinase; JNK, c-Jun NH_2-terminal kinase; ERK, extracellular signal-regulated kinase; DMSO, dimethyl sulfoxide; MTT, 3-(4,5-dimethyl thizol-2-yl)-2,5-diphenyl tetrazolium bromide; CD437, 6-[3-(1-adamantyl)-4-hydroxyphenyl]-2-naphthalene carboxylic acid; LMB, leptomycin B; PD98059, 2-amino-3-methoxyflavone; SP600125, anthra(1,9-*cd*)pyrazol-6(2*H*)-one; PKC, protein kinase C; SB203580, 4-(4-fluorophenyl)-2-(4-methylsulfinylphenyl)-5-(4-pyridyl)1*H*-imidazole; Gö6983, 2-[1-(3-dimethylaminopropyl)-5-methoxyindol-3-yl]-3-(1*H*-indol-3-yl) maleimide; PI3K, phosphatidylinositol-3-kinase; LY294002, 2-(4-morpholinyl)-8-phenyl-4*H*-1-benzopyran-4-one; PARP, poly(ADP-ribose) polymerase; CREB, cAMP response element-binding protein; RT-PCR, reverse transcription-polymerase chain reaction; GAPDH, glyceraldehyde-3-phosphate dehydrogenase; PBS, phosphate-buffered saline; PI, propidium iodide; siRNA, small interfering RNA; AP-1, activator protein-1; CMV, cytomegalovirus; pCMV, phosphorylated cytomegalovirus; C133, CREB133; TV, tumor volume; GBM, glioblastoma multiforme; RTV, relative tumor volume.

rently, conventional chemotherapy for the treatment of advanced tumors, although quite effective, has been associated with adverse events, which is a dose-limited factor. It is clear that new therapeutic options are necessary. Chinese medicine provides novel and efficacious agents for the treatment of a variety of diseases, including those that could not be cured by Western medicine. It was demonstrated that Chinese herbs had antitumoral effects with current chemotherapy in treatment of hepatocellular carcinoma (Yano et al., 1994; Li et al., 2000; Kao et al., 2001).

Angelica sinensis (Oliv.) Diels (AS), also referred to as dong quai or danggui, a traditional Chinese medicine for menopausal symptoms (Yim et al., 2000; Ye et al., 2001a,b), has been clinically administrated for several gynecological symptoms in the United States (Abebe, 2002). In our previous study, the chloroform extract of AS and *N*-butylidenephthalide (BP), derived from the chloroform extract of AS, both revealed dramatic antitumor effects, causing growth arrest and apoptosis of malignant brain tumors in vitro and in vivo (Tsai et al., 2005, 2006). To date, little is known about its antitumor effects on HCC cells.

Nur77 [nerve growth factor (NGF)-induced B or TR3] is a unique transcription factor belonging to the orphan nuclear receptor superfamily (Chang et al., 1989). Unlike other orphan receptors, it is believed that no endogenous ligands are required. In malignant cells such as colon and prostate cancer cells, Nur77 is located in the nucleus and functions as an oncogenic survival factor. Nonetheless, Nur77-caused cell apoptosis via Bcl-2 binding upon administration of certain chemotherapeutic agents induces its migration to mitochondria (Jürgensmeier et al., 1998; Li et al., 2000; Lin et al., 2004). A dominant-negative form of Nur77 that lacks the N-terminal transactivation domain blocks T-cell receptor (TCR)-mediated apoptosis, indicating that Nur77 induction plays a crucial role in the TCR-mediated death of T cells (Woronicz et al., 1994; Winoto, 1997; Winoto and Littman, 2002). Furthermore, the diverse biological activities of Nur77 depend on its subcellular localization. It has been known the induction of Nur77 expression and translocation by antitumorigenic compounds involves members of the mitogen-activated protein kinase (MAPK) family (Kovalovsky et al., 2002; Kolluri et al., 2003). Recent studies have demonstrated that both activation of c-Jun NH_2-terminal kinases (JNK) and inhibition of AKT play a role in translocation of Nur77 from the nucleus to the cytoplasm (Han et al., 2006). In addition, extracellular signal-regulated kinase (ERK) activation plays an important role in cadmium-induced Nur77 expression and apoptosis in lung cancer A549 cells (Shin et al., 2004).

Using oligodeoxynucleotide-based microarray screening, we demonstrated previously that the expression of orphan receptors, including Nurr1, NOR-1, and Nur77, was induced after exposure to BP in brain tumor cells (data not shown). In this study, we characterized the induction of orphan receptor family genes and assessed the possible role of Nur77-induced growth inhibition and apoptosis in vitro and in vivo in HCC cells after treatment with BP. These results distinguish the mode of action of BP from other stimuli and suggest a novel mechanism for understanding the downstream effectors of BP-induced apoptosis in HCC cells.

Materials and Methods

Cell Lines and Cell Culture. The human hepatocellular carcinoma cell line HepG2 (BCRC 60380) was obtained from Bioresources Collection and Research Center (Hsin Chu, Taiwan). The J5 line of human hepatocellular carcinoma cells was kindly provided by Dr. M. J. Chou (Graduate Institute of Basic Medical Science, Chang Gung University, Tao-Yuan, Taiwan, Republic of China). The HepG2 cells were maintained with Dulbecco's modified Eagle's medium containing 10% fetal bovine serum, and the J5 cells were maintained with RPMI 1640 medium containing 10% fetal bovine serum at 37°C in a humidified atmosphere containing 5% CO_2.

Chemicals and Reagents. BP (mol. wt., 188.23) was purchased from Lancaster Synthesis Ltd. (Newgate Morecambe, UK) and dissolved in dimethyl sulfoxide (DMSO) to a concentration of 100 μg/ml and stored at −20°C as a master stock solution. RPMI 1640 medium, Eagle's minimal essential medium, fetal bovine serum, penicillin, streptomycin, trypsin/EDTA, and NuPAGE Bis-Tris electrophoresis system (precast polyacrylamide mini-gel) were purchased from Invitrogen (Carlsbad, CA). RNA isolation kit was purchased from QIAGEN (Valencia, CA). DMSO, 3-(4,5-dimethyl thizol-2-yl)-2,5-diphenyl tetrazolium bromide (MTT), CD437, nuclear export inhibitor leptomycin B (LMB), and horseradish peroxidase-conjugated secondary antibodies were purchased from Sigma-Aldrich (St. Louis, MO). ERK1/2 kinase inhibitor PD98059 and JNK inhibitor SP600125 and phosphor-Bcl-2 (1:500) antibody were purchased from R&D Systems (Minneapolis, MN). Protein kinase C (PKC) inhibitor Gö6983, p38 inhibitor SB203580, and PI3K inhibitor LY294002 were purchased from Calbiochem (San Diego, CA). AKT (1:1000) antibody was purchased from Abcam plc (Cambridge, UK). Nur77 (1:1000), ERK1/2 (1:1000), phosphor-ERK1/2 (1:500). p38 (1:2000), phosphor-p38 (1:1000), JNK (1:1000), phosphor-JNK (1:500), Bcl-2 (1:1000), phosphor-AKT (1:1000), c-Fos, caspase-3 (1:1000), cleaved caspase-3 (1:500), PARP (1:1000), and cleaved PARP (1:500) antibodies were purchased from Cell Signaling Technology Inc. (Danvers, MA). CREB and phosphor-CREB were purchased from Santa Cruz Biotechnology, Inc. Electrophoretic mobility shift assay (EMSA) gel shift kit and nuclear extraction kit were purchased from Panomics Inc. (Redwood, CA). Removal Reagent was from Dainippon Pharmaceutical Co. (Osaka, Japan). Annexin V-FLOUS staining kit was from Roche Molecular Biochemicals (Mannheim, Germany). Polyvinylidene difluoride membranes, bovine serum albumin protein assay kit, and Western blot chemiluminescence reagent were purchased from GE Healthcare (Chalfont St. Giles, Buckinghamshire, UK). Dominant-negative CREB vectors were purchased from BD Biosciences (San Jose, CA).

RT-PCR Analysis. Cells were treated with 50 μg/ml BP for the indicated times (0.5, 1, 3, and 6 h). As treatment control, vehicle (DMSO) was used. After treatment, cells were washed with phosphate-buffered saline, pH 7.4, trypsinized, and scraped from the plate. Total RNA from each sample was isolated by using RNeasy Midi kit and RNase-free DNase set (QIAGEN) according to the manufacturer's protocols. RNA was checked by electrophoresis and ethidium bromide staining on a 1.5% agarose gel. One microgram of total RNA from each sample was used to generate cDNA using the Omniscript RT kit (QIAGEN) according to manufacturer's protocol. One microgram of cDNA was amplified in the presence of 1 μmol of the following primers: Nur77 (F), 5′-CGACCCCCTGACCCCTGAGTT-3′; Nur77 (R), 5′-GCCCTCAAGGTGTTGGAGAAGT-3′; Nurr1 (F), 5′-CGACATTTCTGCCTTCTCC-3′; Nurr1 (R), 5′-GGTAAAGTGTCCAGGAAAAG-3′; NOR-1 (F), 5′-TCTGCCTTCCAAACCAAAG-3′; NOR-1 (R), 5′-TGATGGAAAGTCTGAGGAC-3′; GAPDH (F), 5′-TGAAGGTCGGAGTCAACGGATTTGGT-3′; and GAPDH (R), 5′-CATGTGGGCCATGAGGTCCACCAC-3′, with Taq DNA polymerase (Takara Shuzo Co., Shiga, Japan) (Table 1). The thermal cycling profile was composed of an initial denaturation step at 95°C for 10 min, 35 cycles of 30 s of denaturation at 95°C, 30 s of annealing at

60°C, and 1 min of extension at 72°C, with a final 10-min extension step at 72°C. The intensity of bands was analyzed by GS-800 calibrated imaging densitometer (Quantity One 4.0.3 software; Bio-Rad, Hercules, CA), and levels of GAPDH were used as control.

Cell Fractionation. To investigate whether Nur77 translocates from the nucleus to the cytoplasm., cytoplasmic, nuclear, and mitochondrial fractions were separated by mitochondrial fractionation kit (Active Motif Inc., Carlsbad, CA) according to the manufacturer's instructions. In brief, the J5 cells (5×10^6) were treated with BP in the indicated times. The cells were harvested and washed once with phosphate-buffered saline (PBS). The cells were resuspended for 15 min in ice-cold cytosolic buffer (Active Motif Inc.). On ice, the cells were homogenized using 30 to 50 strokes with a homogenizer. Cells were then sheared by passing them through a 22-gauge needle. The nuclear fraction was recovered by centrifugation at 800*g* for 20 min at 4°C. The "low-speed" pellet was lysed with lysis buffer on ice for 30 min. The low-speed supernatant was centrifuged at 10,000*g* for 20 min at 4°C to obtain the mitochondrial fraction (pellet) and the cytosolic fraction (supernatant). The mitochondrial fraction was further lysed in the mitochondria buffer (Active Motif Inc.) and incubating on ice for 15 min.

Western Blot Analysis. Approximately 5×10^6 cells were cultured in 100-mm^2 dishes and then incubated in various concentrations of isochaihulactone for the indicated times. The cells were lysed on ice with 200 μl of lysis buffer (50 mM Tris-HCl, pH 7.5, 0.5 M NaCl, 5 mM $MgCl_2$, 0.5% Nonidet P-40, 1 mM phenylmethylsulfonyl fluoride, 1 μg/ml pepstatin, and 50 μg/ml leupeptin) and centrifuged at 13,000*g* at 4°C for 20 min. The protein concentrations in the supernatants were quantified using a bovine serum albumin protein assay kit. Electrophoresis was performed on a NuPAGE Bis-Tris electrophoresis system using 50 μg of reduced protein extract per lane. Resolved proteins were then transferred to polyvinylidene difluoride membranes. Filters were blocked with 5% nonfat milk overnight and 1:500 dilutions of primary antibodies for 1 h at room temperature. Membranes were washed with three times with 0.1% Tween 20 and incubated with 1:5000 dilution of horseradish peroxidase-conjugated secondary antibody for 1 h at room temperature. All proteins were detected using Western Lightning Chemiluminescence Reagent Plus kit (PerkinElmer Life and Analytical Sciences, Boston, MA) and quantified using a densitometer.

Growth Inhibition Assay. The viability of the cells after treated with various chemicals was evaluated using MTT assay preformed in triplicate. In brief, the cancer cells (5×10^3) were incubated in 96-well plates containing 200 μl of the culture medium. Cells were permitted to adhere for 12 to 18 h, and then they were washed with PBS. Solutions were always prepared fresh by dissolving 0.2% DMSO or drugs in culture medium and adding the medium to HepG2 and J5 cells. For inhibitor treatment experiments, cells were treated with 50 μg/ml BP and preincubated for 1 h with 25 and 50 μM ERK1/2 kinase inhibitor PD98059, 10 and 20 μM PI3K inhibitor LY294002, or 10 and 20 μM PKC inhibitor Gö6983. After 24 h of exposure, the drug-containing medium was removed, cells were washed with PBS, and replaced with fresh medium. The cells in each well were then incubated in culture medium with 500 μg/ml MTT for 4 h. After the medium was removed, 200 μl of DMSO and 25 μl of glycine buffer (0.1 M glycine and 0.1 M NaCl, pH 10.5) were added to each well. Absorbance at 570 nm of the maximum was detected by a PowerWave X microplate enzyme-linked immunosorbent assay reader (BioTek Instruments, Winooski, VT). The absorbance for DMSO-treated cells was considered as 100%. The results were determined by three independent experiments.

Detection of Apoptosis. Apoptosis was analyzed according to the method described by van Engeland et al. (1998) to detect the integrity of cellular membrane and the externalization of phosphatidylserine (van Engeland et al., 1998). In brief, approximately 10^6 cells were grown in 35-mm-diameter plates. The cells were treated with various herbal extracts and chemicals according to the experimental design and then labeled with 10 μg/ml Annexin V-FLOUS and 20 μg/ml PI before harvesting. After labeling, the cells were washed with binding buffer and harvested by scraping. Cells were resuspended in binding buffer at a concentration of 2×10^5 cells/ml before analysis by flow cytometry (FACScan; BD Biosciences). The data were analyzed on WinMDI software (version 2.8; http://facs.scripps.edu/software.html). The percentage of cells undergoing apoptosis was determined by three independent experiments.

Transfection with siRNA. Nur77 small interfering RNA (siRNA) targeting the sequence 5′-CAG UCC AGC CAU GCU CCU CUU-3′ was synthesized (Ambion, Austin, TX). Cells at 50 to 60% confluence were transfected using GeneJammer transfection reagent (Invitrogen) according to the manufacture's protocol (Stratagene, La Jolla, CA) with Nur77 siRNA (with various concentration of 10–50 nM) for 48 h. Medium was removed, and the cells were treated with BP or vehicle for up to 48 h. After incubation, RNA was isolated for RT-PCR, protein isolated for Western blot, and cells were collected for apoptosis analysis.

Construction of Plasmids. Human Nur77 promoter was isolated using a DNA extraction kit according to the manufacturer's protocol

TABLE 1
Gene-specific primer sequences for reverse-transcription PCR and expected product sizes

Gene & Gene Primer	Sequence	Size
		bp
RT-PCR		
Nurr1		297
Forward	5′-CGACATTTCTGCCTTCTCC-3′	
Reverse	5′-GGTAAAGTGTCCAGGAAAAG-3′	
NOR-1		365
Forward	5′-TCTGCCTTCCAAACCAAAG-3′	
Reverse	5′-TGATGGAAAGTCTGAGGAC-3′	
Nur77		748
Forward	5′-CGACCCCCTGACCCCTGAGTT-3′	
Reverse	5′-GCCCTCAAGGTGTTGGAGAAGT-3′	
GAPDH		965
Forward	5′-TGAAGGTCGGAGTCAACGGATTTGGT-3′	
Reverse	5′-CATGTGGGCCATGAGGTCCACCAC-3′	
Construction of plasmids		
pNur77–496/+67		564
Forward	5′-CGACGCGTGGCTTGGGAAGGTGTAAAGGC-3′	
Reverse	5′-GGAAGATCTCCCAAGTTTCCGTAGCCAC-3′	
pNur77 mut		564
Forward	5′-TCCCTGCGT*TG*ATGGAACCCCGCGTGCGT*TG*CGCGCGCAGA-3′	
Reverse	5′-TCTGCGCGCG*CA*ACGCACGCGGGGTTCCATCAACGCAGG GAG-3′	

bp, base pairs.

(QIAGEN) from volunteer blood. The −496/+67 (pNur77−496/+67) Nur77 promoter regions were generated using the following primers: pNur77−496/+67: sense, 5′-CGACGCGTGGCTTGGGAAGGTGTAAAGGC-3′ and antisenese, 5′-GGAAGATCTCCCAAGTTTCCGTAGCCAC-3′. The amplified product was digested with MluI and BglII restriction enzymes and ligated into pGL3-basic luciferase vector (Promega, Madison, WI) digested with the same enzymes. The AP-1 binding site was mutated using the QuikChange site-mutagenesis kit (Stratagene). For the point mutation of AP-1, sites on the −496/+67 promoter region were generated using the following primers: *pNur77* mut F, 5′-CTCCCTGCGT***TG***ATGGAACCCCGCGTGCGT***TG***CGCGCGCAGA-3′ and *pNur77* mut R, 5′-TCTGCGCGCG***CA***ACGCACGCGGGGTTCCAT***CA***ACGCAGGGAG-3′. Site-specific mutations were confirmed by DNA sequencing.

Transfection of the Luciferase Reporter System. HepG2 and J5 cells were plates in six-well plates at 2×10^5 cells/well in RPMI 1640 medium supplemented with 10% fetal bovine serum. After growth overnight, plasmid mixtures containing 2 μg of Nur77 promoter linked to luciferase and 0.2 μg of pRT-null (Promega) were transfected by GeneJammer reagent according to the manufacturer's protocol. After 48-h transfection, the cells were harvested in 1× luciferase lysis buffer, and luciferase activity was determined and normalized to the pRL-null luciferase activity with a dual-luciferase assay kit (Promega). For the BP treatment, the cells were treated with the drug in the absence of serum for 24 h and then assayed for luciferase activity. The results were determined by three independent experiments.

Electrophoretic Mobility Shift Assay. J5 cells were seeded at 10×10^6 cells per 100-mm dish and incubated with 50 μg/ml BP for 3 h. Nuclear extracts were prepared using the nuclear extraction kit (Panomics Inc.) according to the instructions provided by the manufacturer. The EMSA was performed using a nonradioactive EMSA kit (Panomics Inc.) according to the experimental procedures provided by the manufacturer. In brief, nuclear protein (10 μg) was incubated in binding buffer (10 mM Tris, pH 7.5, 1 mM EDTA, 5 mM $MgCl_2$, 25 mM NaCl, 5% glycerol, 5% sucrose, and 0.01% Nonidet P-40) for 10 min at 37°C. Poly(dI-dC) (3 μg) was added to samples before addition of the oligonucleotide probe. Double-stranded consensus oligonucleotides for the transcription factors AP-1 (5′-CGCTTGATGAGTCAGCCGGAA-3′) were end-labeled with [γ-^{32}P]ATP using T4 polynucleotide kinase, and 1×10^5 counts/min were added to reaction mixtures. For competition studies, 100-fold excess of unlabeled AP-1 oligonucleotide or noncompetitive mutant oligonucleotides 5′-AGTTGAGGCGACTTTCCCAGGC-3′ (nuclear factor-κB mutant) and 5′-CGCTGATATTGGCGGAA-3′ (AP-1 mutant) was added before addition of the radiolabeled probe.

Caspase Activity Assay. Activity of caspase-3 and caspase-9 was detected by using a fluorometric assay kit (Promega) according to the manufacturer's protocol. In brief, 2×10^6 control or treated cells were lysed in 50 μl of cold lysis buffer and incubated in ice for 10 min. Fifty microliters of cell lysates was added to 50 μl of reaction buffer and 5 μl of fluorogenic report substrates specific for caspase-3 or caspase-9 in a 96-well microplate. After incubation at 37°C for 1 h, the fluorescence from the cleaved C-terminal side of the aspartate residue of DEVD-7-amino-4-trifluoromethyl coumarin was detected by a fluorescence microplate reader (Fluoroskan Ascent; Thermo Fisher Scientific, Waltham, MA), with excitation at 400 nm and emission at 505 nm.

CREB Plasmid Transient Transfection. J5 cells were plated in six-well plates at 2×10^5 cells/well in RPMI 1640 medium supplemented with 10% fetal bovine serum. After growth overnight, one of the pCMV (CMV; empty vector), pCMV-CREB (wild type), pCMV-KCREB (K), and pCMV-CREB133 (C133) were transfected by GeneJammer reagent according to the manufacturer's protocol. After 48-h transfection, the cells were treated with 50 μg/ml BP for 1 or 3 h. After 1 h, the cell were harvested and assayed by RT-PCR (for Nur77 RNA expression) and Western blotting (for c-Fos protein expression). The cells were treated with 50 μg/ml BP for 3 h, and then they were harvested and assayed Nur77 protein expression.

Antitumor Activity in Vivo. Xenograft mice were used as a model system to study the cytotoxicity effect of BP in vivo. The implantation of cancer cells was carried out similarly to that described in previous reports. Female congenital athymic BALB/c nude (nu/nu) mice were purchased from National Sciences Council (Taipei, Taiwan), and all procedures were performed in compliance with the standard operating procedures of the Laboratory Animal Center of Tzu Chi University (Hualien, Taiwan). All experiments were carried out using 6- to 8-week-old mice weighing 18 to 22 g. The animals were s.c. implanted with 2×10^6 HepG2 or 5×10^6 J5 cells into their backs. When the tumor reached 80 to 120 mm^3 in volume, animals were divided randomly into control and test groups consisting of six mice per group (day 0). Daily s.c. administration of BP, dissolved in a vehicle consisting of 20% Tween 80 in normal saline (v/v), was performed from days 0 to 4 far from the inoculated tumor sites (>1.5 cm). The control group was treated with vehicle only. The mice were weighed three times a week up to days 21 to 28 to monitor the effects and the same time the tumor volume was determined by measurement of the length and width of the tumor. The tumor volume at day n (TVn) was calculated as TV (cubic millimeters) = (length × $width^2$)/2. The relative tumor volume at day n (RTVn) versus day 0 was expressed according to the following formula: RTVn = TVn/TV0. Tumor regression [T/C (%)] in treated versus control mice was calculated using T/C (%) = (mean RTV of treated group)/(mean RTV of control group) × 100. Xenograft tumors as well as other vital organs of treated and control mice were harvested and fixed in 4% formalin, embedded in paraffin, and cut into 4-mm sections for histologic study.

Immunocytochemistry Staining. J5 cells (1×10^3) were treated with 50 μg/ml BP in the presence or absence of the nuclear export inhibitor LMB at 60 nM. For 3-, 6-, and 12-h incubation, cells were fixation with cold 3.7% formaldehyde. The fixed cells were washed twice in PBS and incubated in cold permeabilization solution (0.1% Triton X-100 and 0.1% sodium citrate). After inactivating endogenous peroxidase with 3% H_2O_2, the cells were washed with PBS again and incubated with an anti-Nur77 antibody at room temperature, followed by an overnight incubation with a 100-fold dilution of anti-Nur77 rabbit polyclonal antibody (Cell Signaling Technology Inc.) in blocking solution. Subsequently, the immune complexes were visualized using the horseradish peroxidase-conjugated anti-goat IgG secondary antibodies (1/1000 dilution; Santa Cruz Biotechnology, Inc.) and LSAB2 system (Dako North America, Inc., Carpinteria, CA), respectively, and then incubated for 10 min with 0.5 mg/ml diaminobenzidine and 0.03% (v/v) H_2O_2 in PBS. Finally, sections were counterstained with hematoxylin, mounted, observed under a light microscope at 400× magnification, and photographed.

Immunohistochemical Staining. All tumor tissues (s.c. HepG2 and J5 tumors with or without BP treatment) were fixed in 4% Formalin at 4°C for 16 h and then embedded in paraffin. Paraffin sections (5 μm) were deparaffinized in xylene and rehydrated through a graded series of ethanol solutions. The sections were incubated with blocking solutions (5% milk power, 1% bovine serum albumin in phosphate-buffered saline) for 60 min at room temperature, followed by an overnight incubation with a 100-fold dilution of anti-Nur77 rabbit polyclonal antibody (Cell Signaling Technology Inc.) in blocking solution. Subsequently, the immune complexes were visualized using the horseradish peroxidase-conjugated anti-goat IgG secondary antibodies (1/1000 dilution; Santa Cruz Biotechnology, Inc.) and LSAB2 system (Dako North America, Inc.), respectively, and then incubated for 10 min with 0.5 mg/ml diaminobenzidine and 0.03% (v/v) H_2O_2 in PBS. Finally, sections were counterstained with hematoxylin, mounted, observed under a light microscope at 400× magnification, and photographed.

Statistical Analysis. The data are shown as mean with standard deviation. The statistical difference was analyzed using the Stu-

dent's t test for normally distributed values and by nonparametric Mann-Whitney U test for values of non-normal distribution. Values of $P < 0.05$ were considered significant.

Results

BP-Related Growth Inhibition and Apoptosis of HCC Cells in Vitro. In our previous studies (Tsai et al., 2005, 2006), we demonstrated the antitumoral effects of BP on glioblastoma multiforme (GBM) brain tumors both in vitro and in vivo. In this study, we selected HepG2 and J5 HCC for further investigations because of its poor prognosis and because it requires a new strategy in clinical practice. MTT assay revealed that BP had a strong antiproliferative effect on HepG2 and J5 cells (Fig. 1A). The IC_{50} value of HepG2 and J5 cells was 25 μg/ml after 48 h of treatment. Compared with untreated cells, BP-treated HepG2 and J5 cells showed obvious cell shrinkage and chromosomal fragmentation typical of cells undergoing apoptosis (data not shown). To elucidate the BP mode of action, the effect of BP on apoptosis was examined. Flow cytometry analysis showed that BP treatment induced apoptosis in a time- and concentration-dependent manner (Fig. 1B).

BP-Induced mRNA and Protein Expression of Nurr1, NOR-1, and Nur77 in HepG2 and J5 Cells and Nur77 Migration from Nucleus to Cytoplasm. To elucidate the mechanism by which BP induces growth inhibition and apoptosis in GBM cells, we used an oligodeoxynucleotide-based microarray screening assay to identify BP-mediated gene expression. Orphan receptor expression, including Nurr1, NOR-1, and Nurr77, was highly induced (data not shown). In this study, the expression of orphan receptors in BP-treated HepG2 and J5 cells was examined, with a focus on the role of BP-induced Nur77 expression. After treatment with BP, mRNA expression of Nurr1, NOR-1, and Nurr77 in both HCC cell lines examined in this study was enhanced in a time-dependent manner, as illustrated in Fig. 2A. Furthermore, the protein expression of Nurr1, NOR-1, and Nur77 was all enhanced in a time-dependent manner. Nurr77 was significantly induced after 3 h of treatment and was maximally expressed 12 h after treatment with BP (Fig. 2B). Because Nur77 migrates from the nucleus to mitochondria to induce apoptosis in response to certain apoptotic stimuli (Yano et al., 1994; Li et al., 2000; Ye et al., 2001a,b), the subcellular localization of Nur77 in J5 was examined. Immunoblotting revealed that Nur77 predominantly localized in the nucleus in the absence of BP treatment. When cells were treated with BP, however, enhanced Nur77 expression in the cytoplasm of J5 cells was noted (Fig. 2C). To further elucidate whether BP-induced translocation of Nur77 was associated with the following apoptosis in J5 cells, LMB, which can specifically inhibit protein exportation from the nucleus (Yoshida et al., 1990; Fornerod et al., 1997) was used. Translocation of Nur77 could be completely blocked by LMB, with Nur77 remaining in the nucleus after 12-h treatment with BP (Fig. 2, D and F). Furthermore, it was also reveled that apoptotic index was only 6.2%, indicating that BP-induced apoptosis was concurrently blocked (Fig. 2F).

BP-Induced J5 cells Apoptosis by Nur77-Mediated Expression. The suppression of Nur77 by Nur77 siRNA was evident in a concentration-dependent manner, as determined

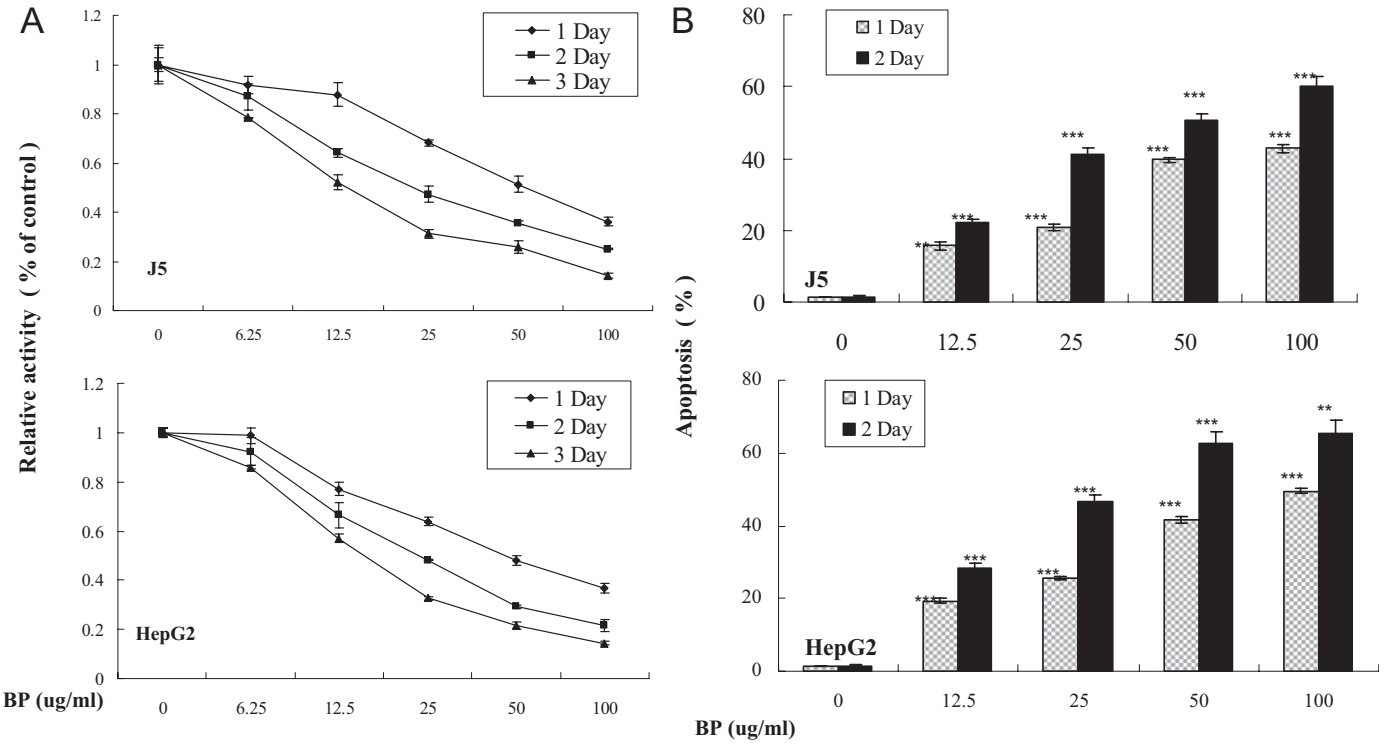

Fig. 1. BP caused growth inhibition of human hepatocellular carcinoma (HCC) cells in vitro and induces apoptosis. A, growth inhibition effect was assessed in human HCC cell lines HepG2 and J5. The cells were treated with various concentrations ranging from 6.25 to 100 μg/ml BP or vehicle (0.2% DMSO) for various times (24, 48, and 72 h) as indicated. Growth inhibition effect (IC_{50}) was determined by MTT assay. The data represent the means ± S.D. of three different experiments. B, cells were treated with various concentrations of 0 to 100 μg/ml BP or vehicle for 24 and 48 h. Cells were collected, and apoptosis was analyzed using PI/Annexin V staining. The data represent the mean and SD from three independent experiments. *, $P < 0.05$; **, $P < 0.01$; ***, $P < 0.001$ versus vehicle.

by RT-PCR (Fig. 3A) and Western blot analysis (Fig. 3B). To further determine the role of Nurr77 in BP-induced apoptosis, flow cytometry analysis was performed to identify the percentage of apoptotic cells after treatment with the siRNA of Nur77. Figure 3C shows that between 70 and 90% of apoptosis was inhibited after treating J5 cells with 50 nM Nur77 siRNA with BP.

To determine whether MAPKs, PKC, or PI3K/AKT/GSK3 play a role in BP-induced growth inhibition of J5 cells, these cells were treated with BP in the presence or absence of the mitogen-activated protein kinase kinase 1/2 inhibitor PD98059, the p38 inhibitor SB203580, JNK1/2 inhibitor SP600125, PKC inhibitor Gö6983, or the PI3K/AKT/GS3K inhibitor LY294002 (10–50 μM). It was shown that PI3K/AKT/GS3K inhibitor LY294002 enhanced BP-induced growth inhibition in a concentration-dependent manner. In contrast, none of the PKC or MAPK inhibitors could abrogate BP-induced growth inhibition in J5 cells (Fig. 3D). To determine which PI3K/AKT/GSK3β pathways were involved in BP-induced growth inhibition, the effect of BP on AKT inhibition was assessed. Inhibition of phosphor-AKT protein expression after exposure of J5 cells to BP. MAPK and PKC protein expression had no obvious changes after drug treatment (Fig. 3E). To investigate a possible role for PI3K/AKT/GSK3β in the regulation of Nur77, J5 cells were treated with BP in the presence or absence of the PI3K inhibitor LY294002. Using Western blot analysis, an inhibition of PI3K and AKT expression with LY294002 enhanced phosphor-Bcl-2 and Nu77 protein levels after treatment with BP was noted (Fig. 3F), suggesting that activation of the PI3K/AKT/GSK3β signaling

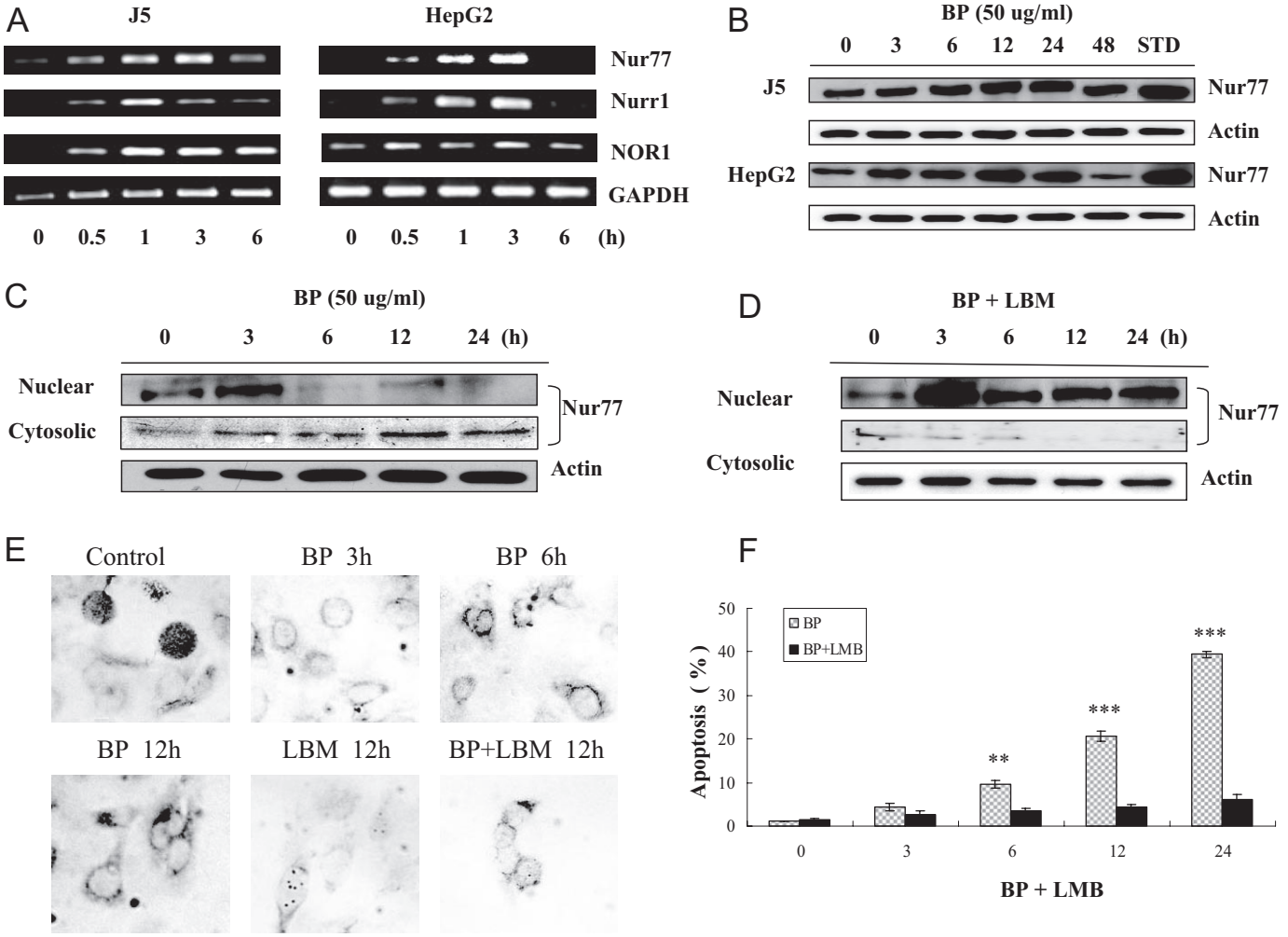

Fig. 2. BP induced mRNA and protein expression of Nurr1, NOR-1, and Nur77 in HepG2 and J5 cells and Nur77 migrated from nucleus to cytoplasm. A, mRNA expression of Nurr1, NOR-1, and Nurr77 in the cells treated with 50 μg/ml BP for various durations (0.5, 1, 3, and 6 h) as indicated. Cells were collected and total RNA isolated for RT-PCR analysis, and expression of GAPDH was used as an internal control. B, protein expressions of Nurr77 in the cells treated with 50 μg/ml BP or vehicle for various durations (3, 6, 12, 24, and 48 h) as indicated. These expressions were assessed by Western blot assay, and expression of β-actin was used as an internal control. STD indicates cell lysate from CD437-treated cells. C, cells treated with 50 μg/ml BP for various duration times (0, 3, 6, 12, and 24 h) as indicated. Nuclear extraction kit (Millipore Bioscience Research Reagents, Temecula, CA) was used for isolation cytoplasm and nucleus. Nur77 expression in both two fractions was evaluated by Western blot analysis, and expression of β-actin was used as an internal control. D, J5 cells (5×10^3) were pretreated with nuclear export inhibitor LMB at 60 nM for 1 h, followed by 50 μg/ml BP for various durations (0, 3, 6, 12, and 24 h) as indicated. Nuclear extraction kit was used for isolation cytoplasm and nucleus. Nur77 expression in both fractions was evaluated by Western blot analysis, and expression of β-actin was used as an internal control. E, J5 cells (1×10^3) were treated with 50 μg/ml BP in the presence or absence of the nuclear export inhibitor LMB at 60 nM. For 3-, 6-, and 12-h incubation, the effect of BP on the Nur77 translocation was determined by immunocytochemistry. The Nur77-positive cells were stained brown (400× magnification). F, J5 cells (5×10^3) were pretreated with nuclear export inhibitor LMB at 60 nM for 1 h, followed by 50 μg/ml BP for various durations (0, 3, 6, 12, and 24 h) as indicated. Cells were collected, and apoptosis was analyzed using PI/Annexin V staining. The data represent the mean and SD from three independent experiments.

pathway may be directed associated with BP-induced Nur77 expression and lead to apoptosis in J5 cells.

BP-Induced Nur77 Expression. To evaluate the importance of the AP1 site of the Nur77 promoter regulating BP-induced Nur77 expression, the pNur77 (−496)/pGL3 deletion Nur77 promoter construct was generated as shown in Fig. 4A). These constructs were transfected into J5 cells and treated with vehicle or BP for 6 h. As an internal control, the plasmid *pRL-TK* (Promega) was used for adjusting transfection efficiency. As illustrated in Fig. 4B, BP treatment resulted in a 30- and 52.5-fold induction of luciferase activity in pNur77 (−496)/pGL3 of HepG2 and J5 cells, respectively. As a control, a pGL3 basic promoterless vector was transfected, and no increase in luciferase activity was noted after BP treatment (Fig. 4B). By pretreating with 20 μM LY294002 for 1 h and then adding 50 μg/ml BP for an additional 24 h, we found that luciferase activity was increased compared with BP treatment alone in HepG2 cells, whereas there was no obvious change in activity in the presence of the PKC inhibitor Gö6983 (Fig. 4C).

Furthermore, by EMSA it is noteworthy that the nuclear extracts from the stimulated cells gave a much stronger band than unstimulated cell extracts after treatment drugs for 3 h. We have proved the AP-1 protein is binding in Nur77 promoter in the presence of BP and PI3K inhibitor LY294002. Competition studies with excess unlabeled oligonucleotide, further demonstrated the specificity of the interaction (Fig. 4D). In addition, c-Fos protein expression was increased in the presence of BP combined LY294002, whereas c-Jun protein expression was not obliviously changed after drug treatment (Fig. 4E).

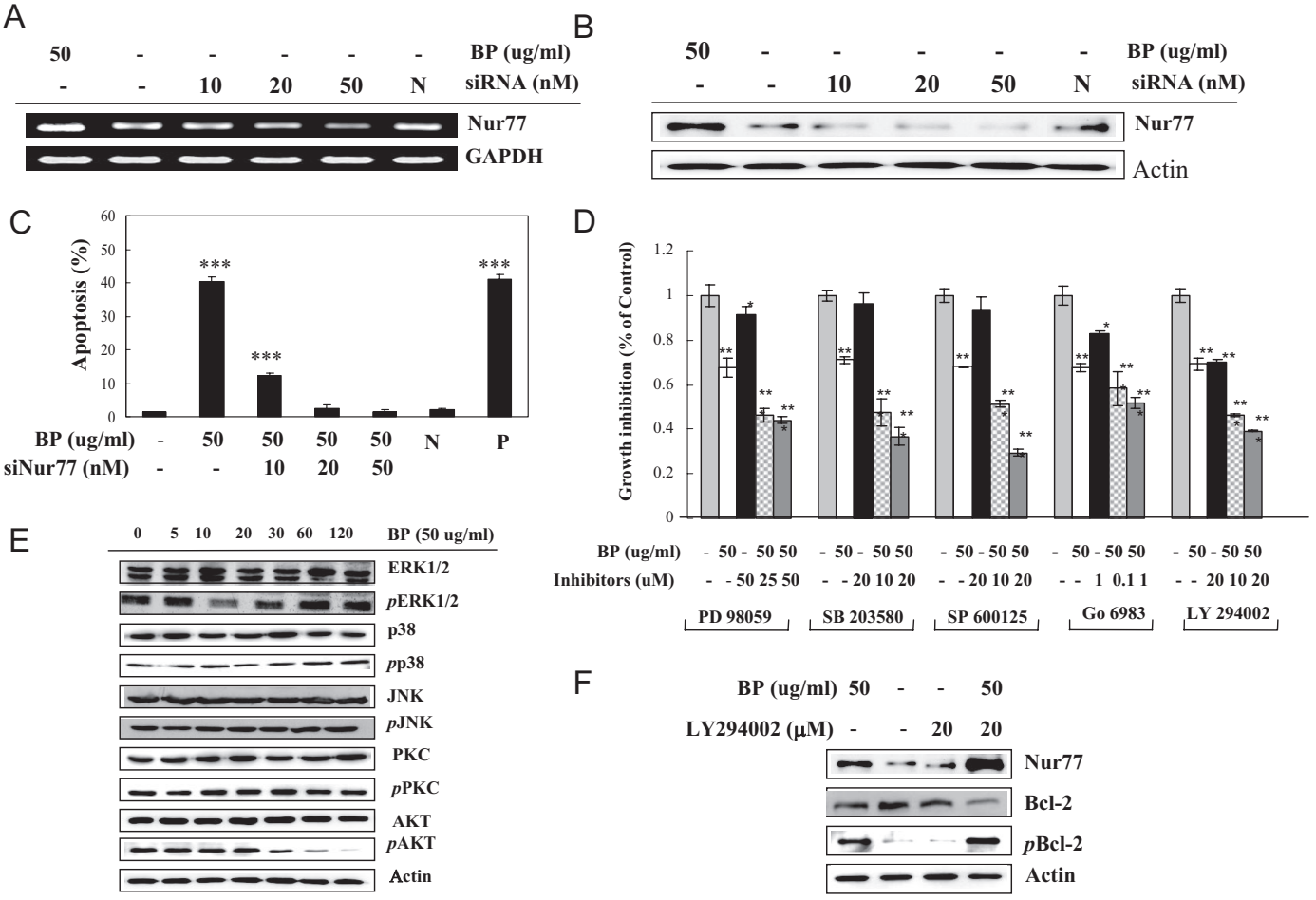

Fig. 3. BP-induced J5 cells apoptosis by Nur77-mediated expression. A, J5 cells were transfected with Nur77 siRNA (siNur77) with various concentrations (10–50 nM) as indicated for 48 h using GeneJammer transfection reagent. RT-PCR was performed for Nur77. Expression of GAPDH was used as an internal control. B, J5 cells were transfected with siNur77, and Western blot analysis was performed for Nur77. Expression of β-actin was used as an internal control. C, siNur77 for various concentrations (10–50 μM) for 48 h using GeneJammer transfection reagent followed by treatment with 50 μg/ml BP or vehicle for 48 h. N, cells transfected with 50 μM Silencer Negative Control siRNA (Ambion). P, cells treated with 10 nM CD437 for 24 h. Cells were collected, and apoptosis was analyzed using PI/Annexin V staining. The data represent the means ± S.D. of three different experiments. *, $P < 0.05$; **, $P < 0.01$; ***, $P < 0.001$ versus vehicle. D, J5 cells (5×10^3) were treated with 50 μg/ml BP in the presence or absence of the mitogen-activated protein kinase kinase 1/2 inhibitor PD98059 (25 and 50 μM), p38 inhibitor SB203580 (10 and 20 μM), JNK1/2 inhibitor SP600125 (10 and 20 μM), PKC inhibitor Gö6983 (10 and 20 μM), or PI3K inhibitor LY294002 (10 and 20 μM). For 24-h incubation, growth inhibition effect was determined by MTT assay. E, J5 cells were treated with BP for various durations (0–120 min) as indicated. Western blot analysis was performed for ERK, phosphor-ERK, p38, phosphor-p38, JNK1/2, phosphor-JNK1/2, PKC, phosphor-PKC, AKT, and phosphor-AKT antibodies. The expression of β-actin was used as an internal control. F, enhancement of phosphor-Bcl-2 expression by PI3K/AKT/GSK3β inhibitor in the BP-induced growth inhibition. J5 cells were in incubated in the presence or absence of the PI3K/AKT/GSK3β inhibitor LY294002 for 1 h and then treated with BP for 12 h. Western blot analysis was performed for Nur77, Bcl-2, and phosphor-Bcl-2, and expression of β-actin was used as an internal control.

BP-Activated Endogenous cAMP-Responsive Gene and BP-Induced Cytotoxicity Was Enhanced by CREB-Dependent Transcriptional Activation. First, to establish the assay system for the transcriptional activation of endogenous cAMP-responsive genes, c-Fos response in the presence of 50 μg/ml BP was investigated. J5 cells were incubated in the presence of 50 μg/ml BP, and expression levels of phosphorylated CREB and c-Fos were analyzed by Western blotting (Fig. 5A). After various times of exposure of J5 cells to BP, both CREB and c-Fos phosphorylations were up-regulated in a time-dependent manner. CREB phosphorylation was induced at 30 min, whereas activation of c-Fos occurred later, beginning at 60 min. Thus, phosphorylated CREB expression was slightly preceded c-Fos by expression. There were no changes in the total amount of CREB in these experiments (Fig. 5A). To confirm that the effect of BP is mediated via the CREB-dependent transcriptional activation, we examined whether the coexpression of expanded BP and dominant-negative CREB blocks the suppressive effect of these compounds. We first confirmed that the transcriptional activation of c-Fos and Nur77 were strongly suppressed in J5 cells expressing dominant-negative CREB vectors (pCMV-CREB133 or pCMV-KCREB) cultured in the presence of 50 μg/ml BP (Fig. 5, B and C). In J5 cells expressing the mutated form of CREB, the BP-induced cytotoxicity was significantly abrogated ($P < 0.001$), confirming CREB

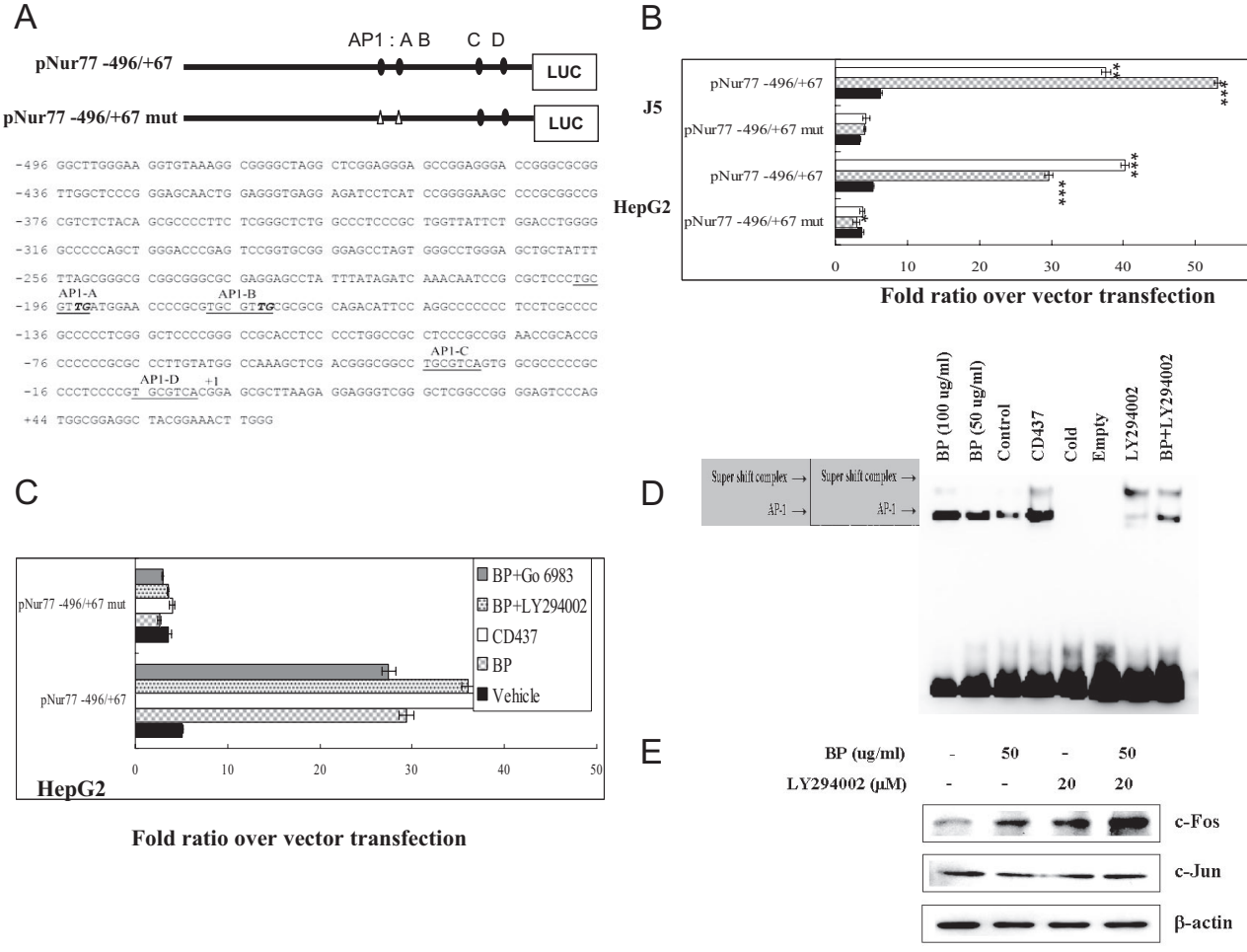

Fig. 4. TCR binding site has an important role in BP-induced Nur77 expression. A, comparison of wild-type and mutant sequence between −496 and +67 in Nur77 promoter region. Mutated base pairs are indicated in each mutated sequence. The constructs of Nur77 promoter vectors with point mutations has been described under *Materials and Methods*. B, Wild-type pNAG−496/+67 or TCR mutant vector (pNur77−496mut12) and pRL-TK cotransfected into HepG2 and J5 cells. These indicated promoter region were fused to luciferase report gene. Each construct (2 μg) was cotransfected with 0.2 μg of pRL-TK vector into HepG2 and J5 cells using GeneJammer transfection reagent followed by treatment with 50 μg/ml BP for 24 h. Cells were lysed, and luciferase activity was measured. Transfection efficiency for luciferase activity was normalized to *Renilla reniformis* luciferase (pRL-TK vector). The *x*-axis shows relative luciferase units [firefly luciferase/*R. reniformis* luciferase (RLU)]. The results show means ± S.D. of three separate transfections. *, $P < 0.05$; **, $P < 0.01$; ***, $P < 0.001$ versus vehicle. C, HepG2 cells were transfected with pNAG−496/+67 reporter plasmid and pRL-TK plasmid. Forty-eight hours after transfection, cells were pretreated with LY294002 for 1 h and then treated with BP for another 24 h. Transfection efficiency for luciferase activity was normalized to *R. reniformis* luciferase (pRL-TK vector). The *x*-axis shows relative luciferase units (RLU). The results show means ± S.D. of three separate transfection. D, EMSA analysis of LY294002 and BP stimulation of AP-1 complex formation. Ten micrograms of nuclear protein extracted from untreated (control), LY294002 (LY294002), BP-treated (BP), and LY204002 combined BP-treated J5 cells was incubated with an AP-1, double-stranded oligonucleotide as described under *Materials and Methods* (In combined treatment experiments, J5 cells were in incubated in the presence of the PI3K/AKT/GSK3β inhibitor LY294002 for 1 h and then treated with BP for 12 h.) Binding reactions carried out with the addition of excess (100-fold) unlabeled probe resulted in complete elimination of binding complexes in both control and treated conditions. E, enhancement of c-Fos expression by PI3K/AKT/GSK3β inhibitor in the BP-induced growth inhibition. J5 cells were in incubated in the presence or absence of the PI3K/AKT/GSK3β inhibitor LY294002 for 1 h and then treated with BP for 3 h. Western blot analysis was performed for c-Fos, c-Jun, and expression of β-actin was used as an internal control.

involvement in the suppression of expanded BP-induced cytotoxicity (Fig. 5D).

BP-Induced Mitiochondria-Dependent Apoptosis in J5 Cells. To examine whether Nur77 results in cytochrome *c* release after treatment with BP in J5 cells, mitochondria enriched by cytosol/mitochondria fractionation kit was used. In this study, it was noted that cytochrome *c* migrated from the mitochondria to the cytoplasm after drug treatment in a time-dependent manner (Fig. 6A). As shown in Fig. 6B, caspase-9 and caspase-3 were both activated in a time-dependent manner using specific fluorogenic peptide substrates after addition of 50 μg/ml BP to J5 cells. Because activation of the caspases and cleavage of PARP are crucial mechanisms for induction of apoptosis and initiator caspases (e.g., caspase-1, -2, -8, -9, and -10) are involved in the early stages of the proteolytic cascade, their involvement in BP-induced apoptosis was investigated in J5 cells. It was evidenced that BP-induced apoptosis is associated with activation of caspase-3 and PARP in a time-dependent manner (Fig. 6C). Otherwise, these results indicated that BP might be related to mitochondria-dependent apoptosis pathway in J5 cells.

BP-Induced in Vivo Growth Inhibition of HepG2 and J5 Xenografts in Nude Mice. To evaluate the antitumor activity of BP in vivo, human liver cancer xenografts were established by s.c. injection of approximately 2×10^6 HepG2 and 5×10^6 J5 into the dorsal subcutaneous tissue and cells on the backs of nude mice. After the tumor reached approximately 100 to 250 mm^3, mice were randomized into vehicle control and treatment groups (six animals each) and given a daily s.c. injection of either 0 (control group) or 50, 100, 300, and 500 mg/kg BP (treatment groups) for five successive days.

Significant suppression of tumor growth was observed in the BP-50, BP-100, BP-300, and BP-500-treated groups compared with the control group. Besides, overexpression of Nur77 protein in the developing tumor was confirmed by Western blot analysis with BP-treated tumor cells (Fig. 7, A and B). There were no significant differences between the control and BP-treated groups with respect to the body weight of the animals (data not shown). Nur77 and caspase-3 expression were up-regulated in the human HepG2 and J5 tumor tissues treated with BP relative to the control group at day 10 after treatment (Fig. 7C).

Discussion

In our previous study, we examined BP-induced changes in gene expression within GBM brain tumor cells using an oligodeoxynucleotide-based microarray assay. In this study, Nur77 was the gene of interest because it is involved in the apoptotic processes of a variety of cells and tissues, as well as being an immediate-early-response gene induced by growth factors and mitogens (Nakai et al., 1990; Youn et al., 2000). Nur77 is also rapidly induced by TCR signaling in immature thymocytes and T-cell hybridomas, as well as tumor cells of the lung, prostate, ovary, colon, and stomach (Liu et al., 1994;

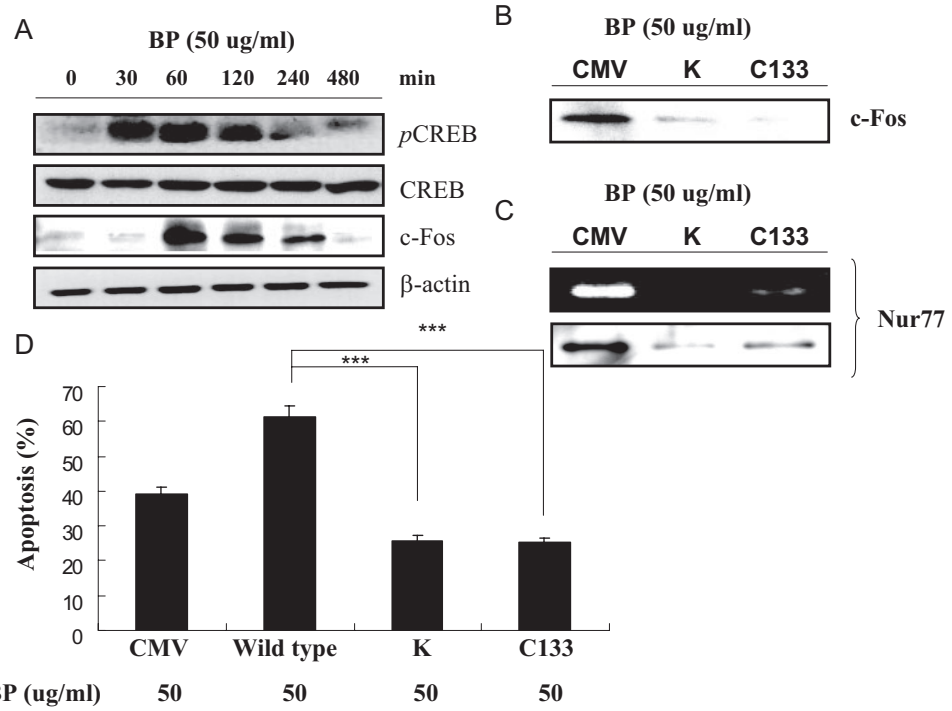

Fig. 5. Phosphorylation of CREB and transcriptional activation of Nur77 were strongly enhanced by BP treatment. A, J5 cells were treated with BP for various durations (0–480 min) as indicated. Western blot analysis was performed for phosphor-CREB, CREB, and c-Fos antibodies. The expression of β-actin was used as an internal control. (B) J5 cells were transfected with one of the pCMV (CMV; empty vector), pCMV-KCREB (K), and pCMV-CREB133 (C133) and incubated in the presence of 50 μg/ml BP for 1 h. Western blot analysis was performed for c-Fos antibody. C, J5 cells were transfected with one of the pCMV (CMV; empty vector), pCMV-KCREB (K), and pCMV-CREB133 (C133) and incubated in the presence of 50 μg/ml BP. Top, J5 cells were treated with BP for 1 h, and RT-PCR was used to evaluate Nur77 mRNA expression. Bottom, J5 cells were treated with BP for 3 h, and Western blot was used to estimate for the Nur77 protein expression. D, J5 cells were transfected with one of the pCMV (CMV; empty vector), pCMV-CREB (wild type), pCMV-KCREB (K), and pCMV-CREB133 (C133). These cells were treated with 50 μg/ml BP for 48 h. Cells were collected, and apoptosis was analyzed using PI/Annexin V staining. The data represent the mean and SD from three independent experiments. *, $P < 0.05$; **, $P < 0.01$; ***, $P < 0.001$ versus vehicle.

MOL PHARM
MOLECULAR PHARMACOLOGY
aspet

Uemura et al., 1998; Stocco et al., 2002; Wilson et al., 2003; Wu et al., 2003; Shin et al., 2004).

To investigate whether BP-induced overexpression of Nur77 is involved in HCC cell apoptosis, Nur77 mRNA and protein induction after BP treatment was evaluated in both HepG2 and J5 cell lines. Nur77 protein translocation from the nucleus to cytoplasm was also studied. In both HepG2 and J5 cells, BP-induced Nur77 protein expression was increased 3 h after BP treatment, with expression being highest after 12 h. Nur77 protein translocation was observed after 6 h of BP treatment. In addition, after the activation of caspase 9 and caspase 3, cytochrome *c* was detected in the J5 cytoplasm after BP treatment. In cancer cells, it is known that Nur77 functions in the nucleus as an oncogenic survival factor. In response to apoptotic stimuli, Nur77 translocates from the nucleus to the cytoplasm, where it binds to Bcl-2, triggering cytochrome *c* release and apoptosis (Li et al., 2000). Because inhibition of Nur77 expression and blockade of Nur77 translocation into cytoplasm with siRNA abrogated BP-induced apoptosis, it is possible that Nur77 has a role in BP-induced apoptotic cell death. Moreover, an antitumor effect of BP in a nude mouse xenograft animal model has been reported in which expression of Nur77 is associated with the antitumor activity of BP. Together, these results suggest that the antitumor activity of BP is mediated via Nur77 and that Nur77 might play a role of BP on antitumor effect in HCC cells.

The induction of Nur77 expression has been reported in other cell types as well. Nur77 expression was rapidly induced by nerve growth factor in PC 12 cells via Ca^{2+} (Milbrandt, 1988; Katagiri et al., 1997), by cadmium in human lung cell lines via extracellular signal-regulated kinase and protein kinase A (Shin et al., 2004), and by PGF2a and Butaprost in human embryonic kidney 293/EBMA via protein kinase C (Liang et al., 2004). In addition, a recent report implicates both activation of JNK and inhibition of AKT in the translocation of Nur77 from the nucleus to the cytoplasm in other cancer models (Han et al., 2006). Thus, regulation of Nur77 expression may involve diverse intracellular mechanisms that are dependent upon different stimuli. It has been demonstrated that the PI3K inhibitors wortmannin and LY294002 stimulate stress-activated protein kinase/JNK and p38 phosphorylation, in a manner that parallels the inhibition of protein kinase B (AKT) phosphorylation. Fur-

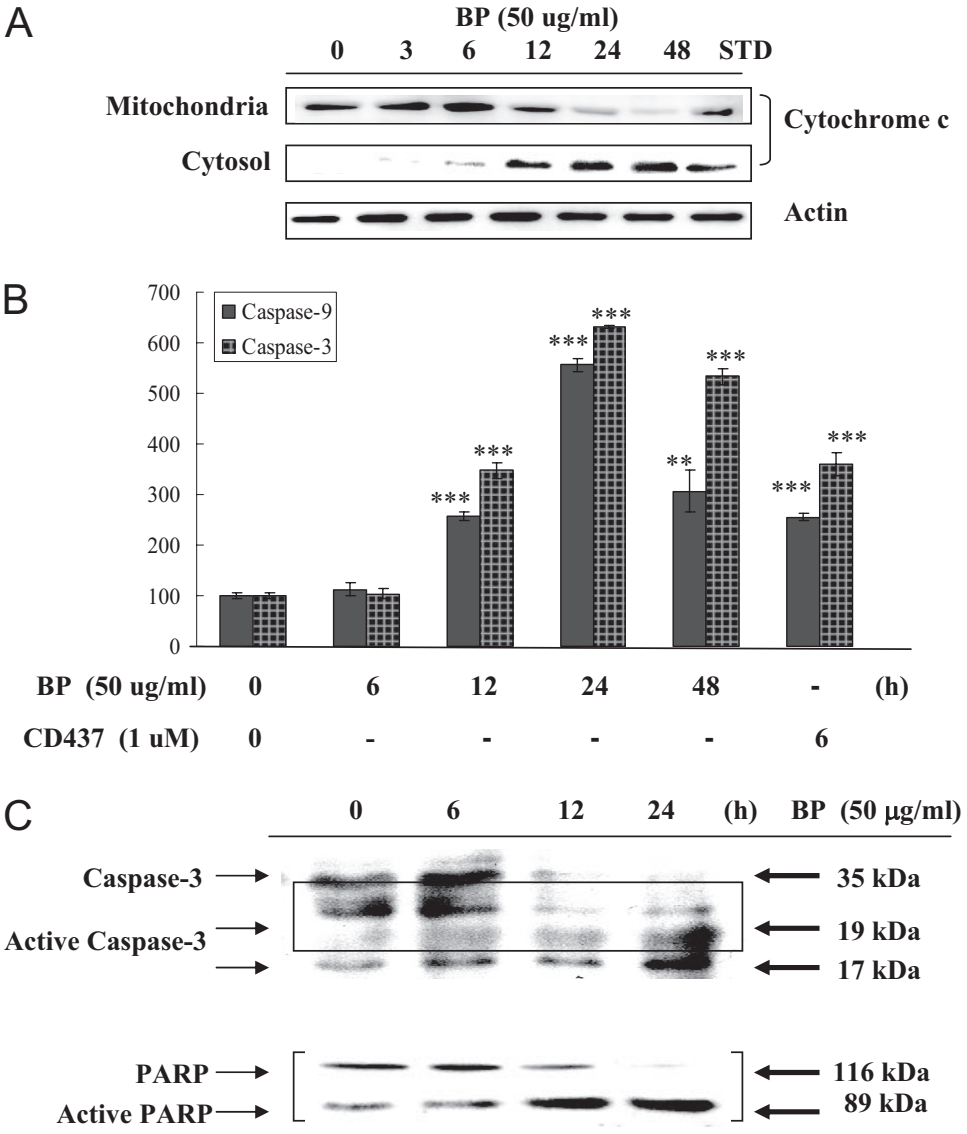

Fig. 6. BP induced mitochondria-dependent apoptosis in J5 cells. A, cytochrome *c* release from mitochondria assessed by Western blot assay. The cells treated with 50 μg/ml BP for various durations (0, 3, 6, 12, 24, and 48 h) as indicated. Mitochondria enriched using cytosol/mitochondria fractionation kit (Calbiochem). Cytochrome *c* expression in both fractions was evaluated by Western blot analysis, and expression of β-actin was used as an internal control. STD indicates cell lysate from CD437-treated cells. B, J5 cells were treated with 50 μg/ml BP for various durations (6, 12, 24, and 48 h) as indicated. The *y*-axis shows relative caspase-9 and caspse-3 activity. The data represent the means ± S.D. of three different experiments. *, $P < 0.05$; **, $P < 0.01$; ***, $P < 0.001$ versus vehicle. C, J5 cells were treated with BP for various durations (6, 12, and 24 h) as indicated. Western blot analysis was performed for caspase-3, cleaved caspase-3, PARP, and cleaved PARP. The expression of β-actin was used as an internal control.

thermore, it has been shown by EMSA and supershift analysis that wortmannin stimulates AP-1 complex formation (Sidhu et al., 2001). In addition, it has been reported that intrathecal pretreatment with wortmannin and LY294002 produced a dose-dependent increase in naloxone-precipitated jumping, which was accompanied by an increase in expression of spinal Fos protein in both acute and chronic morphine-dependent mice (Yang et al., 2006).

In this study, we found that BP inhibits AKT protein phosphorylation (Fig. 3E) and that BP has a synergistically cytotoxic effect with LY294002 (Fig. 3D).

There are some potential *cis*-acting elements in the Nur77 promoter region. A region from −496 to −334 was identified that contains enhancers that are responsive to prostaglandin $F_{2\alpha}$ and Butaprost through the PKC pathway (Liang et al., 2004). The major PKC signal response element in the Nur77 promoter is an AP-1-like element (Kim et al., 2005), whereas a Nur77 promoter (−496 to +67) containing four AP-1 motifs has also been reported (Uemura et al., 1995). To consider whether the AP-1 motif is involved in the PI3K/AKT/GSK3β signaling pathway, as well as further studying the transcription mechanisms of BP-mediated Nur77 mRNA expression, a Nur77 promoter (−496 to +67) containing these four AP-1 motifs was subcloned into a luciferase reporter plasmid. We found that BP-induced a 30- and 50.2-fold increase in the luciferase activity of HepG2 and J5 cells, respectively, compared with the vehicle control. To investigate whether these AP-1 motifs are functional BP motifs, the protocol of Kim et al. (2005) was used to mutate two AP-1 motifs (−197 to −192; −179 to −173) within the Nur77 promoter. Mutation of the AP-1 motif resulted in a dramatic decrease of BP-induced Nur77 promoter activity. By pretreating with 20 μM LY294002 for 1 h and then adding 50 μg/ml BP for an additional 24 h, we found that luciferase activity was increased compared with BP treatment alone in HepG2 cells, whereas there was no obvious change in activity in the presence of the PKC inhibitor Gö6983 (Fig. 4C).

As indicated by EMSA, nuclear extracts from stimulated cells gave a much stronger binding than unstimulated cell extracts after treatment for 3 h. Here, we demonstrated that

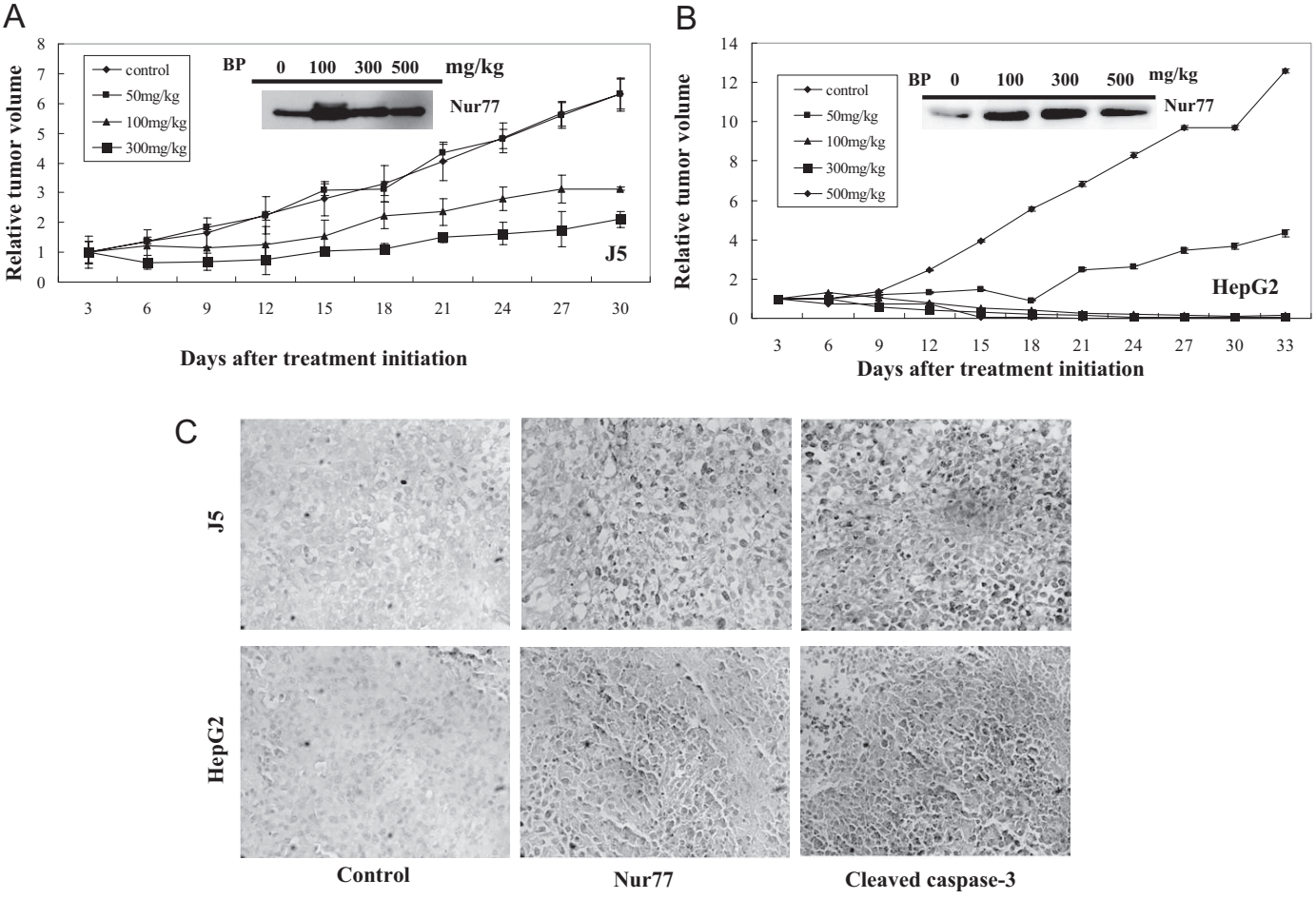

Fig. 7. BP-induced in vivo growth inhibition of HepG2 and J5 xenografts in nude mice. Inhibition of tumor growth from HepG2 and J5 cells that overexpression Nur77 protein. A and B, nude mice were injected with approximately 2×10^6 HepG2 or 5×10^6 J5 into the dorsal subcutaneous tissue. When the tumor volumes reached 100 to 250 mm^3, HepG2 and J5 tumor-bearing mice were administered s.c. with vehicle control (♦), 50 mg/kg (small ■), 100 mg/kg (▲), 300 mg/kg (large ■), or 500 mg/kg (*) BP on days 0 to 4 for 5 days. The figures show the relative tumor volume and Nur77 protein expression in HepG2 and J5 tumor cells of control and therapeutic groups. Data represent means ± S.D. of tumor volume and body weight at each time point. Expressions of Nur77 and caspase-3 in HepG2 and J5 xenografts are shown. Nude mice were injected with approximately 2×10^6 HepG2 or 5×10^6 J5 into the dorsal subcutaneous tissue. When the tumor volumes reached 50 to 100 mm^3, HepG2 and J5 tumor-bearing mice were administered s.c. with vehicle control (♦) or 100 mg/kg (■) for 5 days. Five days later, tumors were homogenized for protein extraction. C, representative photographs of sections of the control group and BP-treated group HepG2 and J5 tumors, immunohistochemically stained with Nur77 and caspase-3 rabbit polyclonal antibodies. The Nur77 and cleaved caspase-3-positive cells were stained brown (400× magnification). Scale bars, 100 μm.

AP-1 protein will bind to the Nur77 promoter in the presence of either BP or LY294002. Competition studies with excess unlabeled oligonucleotide further demonstrated the specificity of the interaction. In addition, c-Fos protein expression was increased in the presence of BP combined with LY294002, whereas c-Jun protein expression was not significantly changed after drug treatment. These results suggest that AP-1 may be involved in BP and LY294002-induced Nur77 protein expression. As shown by EMSA, there is a supershift complex formation after BP and LY294002 treatment. At present, we suggest that c-Fos up-regulation might result from this supershift complex formation. These results demonstrate that Nur77 activation is probably enhanced by exposure of HCC cells to LY294002. It is known that CREB is phosphorylated by several stimuli, including Ca^{2+} and cAMP, and then leads to c-Fos activation (Taurin et al., 2002; Wiggin et al., 2002; Barlow et al., 2006; Lee et al., 2007). To examine whether the c-Fos induction of BP was due to CREB activation, Western blotting for CREB phosphorylation and dominant-negative CREB transfection analysis were used. After various exposure times of J5 cells to BP, both CREB and c-Fos phosphorylation were up-regulated in a time-dependent manner. CREB phosphorylation was induced at 30 min, whereas c-Fos phosphorylation occurred later, beginning at 60 min (Fig. 5A). We then confirmed that the transcriptional activation of c-Fos and Nur77 was obviously inhibited in J5 cells expressing dominant-negative CREB vectors (Fig. 5, B and C). Furthermore, we transfected J5 cells with one of the dominant-negative CREB vectors, and we found that the expression of dominant-negative CREB blocks the apoptosis effect of BP in the presence of BP 24 h (Fig. 5D). It was been demonstrated that nerve growth factor and agents that trigger an increase in intracellular levels of cAMP or Ca^{2+} induce the phosphorylation of CREB Ser-133 to a similar extent, these stimuli influence the transcription of genes containing cAMP response elements in distinct ways. It is noteworthy that dominant-negative CREB has been shown to completely inhibit the cAMP-induced *c-fos* gene (Ahn et al., 1998). As mentioned, Nur77 expression was rapidly induced by NGF in PC-12 cells via Ca^{2+} (Milbrandt, 1988; Katagiri et al., 1997). Therefore, a novel finding in this study was not only c-Fos but also CREB phosphorylation in response to BP-induced Nur77 expression. Although the mechanism of activation of CREB phosphorylation needs further study, the observation that CREB phosphorylation precedes c-Fos expression after treatment with BP is probably attributable to the BP-induced growth inhibition.

Until now, the synergistically cytotoxic effect caused by BP and LY294002 is perhaps directly associated with Nur77 protein overexpression and translocation to cytoplasm in HCC cells. This phenomenon should lead to greater inhibition of Bcl-2 and thereby enhanced apoptosis. The critical role of subsequent Nur77 redistribution reveals a novel cross-talk between orphan receptors and their behavior in promoting apoptosis in J5 cells through PI3K/AKT/GSK3β signal transduction. Together, these results indicate that AP-1 motif is crucial for BP-induced Nur77 mRNA expression. This phenomenon showed that PI3K inhibition might be related to Nur77 activation and lead to apoptosis.

In summary, the mechanisms underlying the antitumor activity of BP were studied. Our previous studies showed growth inhibition and antitumor activity in a variety of tumor cell lines in vitro and inhibition of xenografts, including GBM brain tumor cells, in vivo (Tsai et al., 2005, 2006). In this study, it was shown that when HCC cells are exposed to BP, Nur77 is the gene that increases expression the most and the PI3K/AKT/GSK3β signaling pathways have been implicated in the regulation of BP-induced apoptosis. These results suggest a gene target for BP, which may be useful for future clinical applications.

References

Abebe W (2002) Herbal medication: potential for adverse interactions with analgesic drugs. *J Clin Pharm Ther* **27:**391–401.

Ahn S, Olive M, Aggarwal S, Krylov D, Ginty DD, and Vinson C (1998) A dominant-negative inhibitor of CREB reveals that it is a general mediator of stimulus-dependent transcription of c-fos. *Mol Cell Biol* **18:**967–977.

Barlow CA, Shukla A, Mossman BT, and Lounsbury KM (2006) Oxidative-mediated cAMP response element binding protein activation: calcium regulation and role in apoptosis of lung epithelial cells. *Am J Respir Cell Mol Biol* **34:**7–14.

Chang C, Kokontis J, Liao SS, and Chang Y (1989) Isolation and characterization of human TR3 receptor: a member of steroid receptor superfamily. *J Steroid Biochem* **34:**391–395.

Fornerod M, Ohno M, Yoshida M, and Mattaj IW (1997) CRM1 is an export receptor for leucine-rich nuclear export signals. *Cell* **90:**1051–1060.

Han YH, Cao X, Lin B, Lin F, Kolluri SK, Stebbins J, Reed JC, Dawson MI, and Zhang XK (2006) Regulation of Nur77 nuclear export by c-Jun N-terminal kinase and Akt. *Oncogene* **25:**2974–2986.

Jürgensmeier JM, Xie Z, Deveraux Q, Ellerby L, Bredesen D, and Reed JC (1998) Bax directly induces release of cytochrome c from isolated mitochondria. *Proc Natl Acad Sci U S A* **95:**4997–5002.

Kao ST, Yeh CC, Hsieh CC, Yang MD, Lee MR, Liu HS, and Lin JG (2001) The Chinese medicine Bu-Zhong-Yi-Qi-Tang inhibited proliferation of hepatoma cell lines by inducing apoptosis via G0/G1 arrest. *Life Sci* **69:**1485–1496.

Katagiri Y, Hirata Y, Milbrandt J, and Guroff G (1997) Differential regulation of the transcriptional activity of the orphan nuclear receptor NGFI-B by membrane depolarization and nerve growth factor. *J Biol Chem* **272:**31278–31284.

Kim H, Lee JE, Kim BY, Cho EJ, Kim ST, and Youn HD (2005) Menin represses JunD transcriptional activity in protein kinase C theta-mediated Nur77 expression. *Exp Mol Med* **37:**466–475.

Kolluri SK, Bruey-Sedano N, Cao X, Lin B, Lin F, Han YH, Dawson MI, and Zhang XK (2003) Mitogenic effect of orphan receptor TR3 and its regulation by MEKK1 in lung cancer cells. *Mol Cell Biol* **23:**8651–8667.

Kovalovsky D, Refojo D, Liberman AC, Hochbaum D, Pereda MP, Coso OA, Stalla GK, Holsboer F, and Arzt E (2002) Activation and induction of NUR77/NURR1 in corticotrophs by CRH/cAMP: involvement of calcium, protein kinase A, and MAPK pathways. *Mol Endocrinol* **16:**1638–1651.

Lee J, Rushlow WJ, and Rajakumar N (2007) L-type calcium channel blockade on haloperidol-induced c-Fos expression in the striatum. *Neuroscience* **149:**602–616.

Li H, Kolluri SK, Gu J, Dawson MI, Cao X, Hobbs PD, Lin B, Chen G, Lu J, Lin F, et al. (2000) Cytochrome c release and apoptosis induced by mitochondrial targeting of nuclear orphan receptor TR3. *Science* **289:**1159–1164.

Li XK, Motwani M, Tong W, Bornmann W, and Schwartz GK (2000) Huanglian, a chinese herbal extract, inhibits cell growth by suppressing the expression of cyclin B1 and inhibiting CDC2 kinase activity in human cancer cells. *Mol Pharmacol* **58:**1287–1293.

Liang Y, Li C, Guzman VM, Chang WW, Evinger AJ, Pablo JV, and Woodward DF (2004) Upregulation of orphan nuclear receptor Nur77 following PGF2a, bimatoprost, and butaprost treatments. Essential role of a protein kinase C pathway involved in EP2 receptor activated Nur77 gene transcription. *Br J Pharmacol* **142:**737–748.

Lin B, Kolluri SK, Lin F, Liu W, Han YH, Cao X, Dawson MI, Reed JC, and Zhang XK (2004) Conversion of Bcl-2 from protector to killer by interaction with nuclear orphan receptor Nur77/TR3. *Cell* **116:**527–540.

Liu ZG, Smith SW, McLaughlin KA, Schwartz LM, and Osborne BA (1994) Apoptotic signals delivered through the T-cell receptor of a T-cell hybrid require the immediate-early gene nur77. *Nature* **367:**281–284.

Milbrandt J (1988) Nerve growth factor induces a gene homologous to the glucocorticoid receptor gene. *Neuron* **1:**183–188.

Nakai A, Kartha S, Sakurai A, Toback FG, and DeGroot LJ (1990) A human early response gene homologous to murine nur77 and rat NGFI-B, and related to the nuclear receptor superfamily. *Mol Endocrinol* **4:**1438–1443.

Shin HJ, Lee BH, Yeo MG, Oh SH, Park JD, Park KK, Chung JH, Moon CK, and Lee MO (2004) Induction of orphan nuclear receptor Nur77 gene expression and its role in cadmium-induced apoptosis in lung. *Carcinogenesis* **25:**1467–1475.

Sidhu JS, Liu F, Boyle SM, and Omiecinski CJ (2001) PI3K inhibitors reverse the suppressive actions of insulin on CYP2E1 expression by activating stress-response pathways in primary rat hepatocytes. *Mol Pharmacol* **25:**1138–1146.

Stocco CO, Lau LF, and Gibori G (2002) A calcium/calmodulin-dependent activation of ERK1/2 mediates JunD phosphorylation and induction of nur77 and 20α-hsd genes by prostaglandin F2α in ovarian cells. *J Biol Chem* **277:**3293–3302.

Taurin S, Dulin NO, Pchejetski D, Grygorczyk R, Tremblay J, Hamet P, and Orlov SN (2002) c-Fos expression in ouabain-treated vascular smooth muscle cells from rat aorta: evidence for an intracellular-sodium-mediated, calcium-independent mechanism. *J Physiol* **15:**835–847.

Tsai NM, Lin SZ, Lee CC, Chen SP, Su HC, Chang WL, and Harn HJ (2005) The antitumor effects of *Angelica sinensis* on malignant brain tumors in vitro and in vivo. *Clin Cancer Res* **11:**3475–3484.
Tsai NM, Chen YL, Lee CC, Lin PC, Cheng YL, Chang WL, Lin SZ, and Harn HJ (2006) The natural compound n-butylidenephthalide derived from *Angelica sinensis* inhibits malignant brain tumor growth in vitro and in vivo. *J Neurochem* **99:**1251–1262.
Uemura H, Mizokami A, and Chang C (1995) Identification of a new enhancer in the promoter region of human TR3 orphan receptor gene. A member of steroid receptor superfamily. *J Biol Chem* **270:**5427–5433.
van Engeland M, Nieland LJ, Ramaekers FC, Schutte B, and Reutelingsperger CP (1998) Annexin V-affinity assay: a review on an apoptosis detection system based on phosphatidylserine exposure. *Cytometry* **31:**1–9.
Wiggin GR, Soloaga A, Foster JM, Murray-Tait V, Cohen P, and Arthur JS (2002) MSK1 and MSK2 are required for the mitogen- and stress-induced phosphorylation of CREB and ATF1 in fibroblasts. *Mol Cell Biol* **22:**2871–2881.
Wilson AJ, Arango D, Mariadason JM, Heerdt BG, and Augenlicht LH (2003) TR3/Nur77 in colon cancer cell apoptosis. *Cancer Res* **63:**5401–5407.
Winoto A (1997) Genes involved in T-cell receptor-mediated apoptosis of thymocytes and T-cell hybridomas. *Semin Immunol* **9:**51–58.
Winoto A and Littman DR (2002) Nuclear hormone receptors in T lymphocytes. *Cell* **109 (Suppl):**57–66.
Woronicz JD, Calnan B, Ngo V, and Winoto A (1994) Requirement for the orphan steroid receptor Nur77 in apoptosis of T-cell hybridomas. *Nature* **367:**277–281.
Wu Q, Liu S, Ye XF, Huang ZW, and Su WJ (2003) Dual roles of Nur77 in selective regulation of apoptosis and cell cycle by TPA and ATRA in gastric cancer cells. *Carcinogenesis* **23:**1583–1592.
Yang L, Zhu CJ, Cao JL, and Zeng YM (2006) Inhibition of the spinal phosphoinositide 3-kinase exacerbates morphine withdrawal response. *Neurosci Lett* **404:** 237–241.
Yano H, Mizoguchi A, Fukuda K, Haramaki M, Ogasawara S, Momosaki S, and Kojiro M (1994) The herbal medicine sho-saiko-to inhibits proliferation of cancer cell lines by inducing apoptosis and arrest at the G0/G1 phase. *Cancer Res* **54:**448–454.
Ye YN, Koo MW, Li Y, Matsui H, and Cho CH (2001a) *Angelica sinensis* modulates migration and proliferation of gastric epithelial cells. *Life Sci* **68:**961–968.
Ye YN, Liu ES, Li Y, So HL, Cho CC, Sheng HP, Lee SS, and Cho CH (2001b) Protective effect of polysaccharides-enriched fraction from *Angelica sinensis* on hepatic injury. *Life Sci* **69:**637–646.
Yim TK, Wu WK, Pak WF, Mak DH, Liang SM, and Ko KM (2000) Myocardial protection against ischaemia-reperfusion injury by a *Polygonum multiflorum* extract supplemented 'Dang-Gui decoction for enriching blood', a compound formulation, ex vivo. *Phytother Res* **14:**195–199.
Yoshida M, Nishikawa M, Nishi K, Abe K, Horinouchi S, and Beppu T (1990) Effects of leptomycin B on the cell cycle of fibroblasts and fission yeast cells. *Exp Cell Res* **187:**150–156.
Youn HD, Chatila TA, and Liu JO (2000) Integration of calcineurin and MEF2 signals by the coactivator p300 during T-cell apoptosis. *EMBO J* **19:**4323–4331.

Address correspondence to: Dr. Horng-Jyh Harn, Department of Pathology, China Medical University and Hospital, 2, Yude Rd., North District, Taichung 40447, Taiwan, Republic of China. E-mail: dukeharn@www.cmuh.org.tw